Water speciation in rhyolitic melt determined by in-situ infrared spectroscopy

John R. Sowerby* and Hans Keppler

Bayerisches Geoinstitut, Universität Bayreuth, D-95440 Bayreuth, Germany

Abstract

Near-IR spectra obtained from hydrous silicate melts, close to natural rhyolite, were acquired at both high temperature using a heating stage and simultaneously at high pressure and temperature using a hydrothermal diamond cell. The temperature dependence of the extinction coefficients for the peaks due to OH and H_2O is negligible. In both sets of experiments, the speciation reaction H_2O + O = 2OH is shifted to the right with increasing temperature above the glass transition but changes below this are negligible, within experimental uncertainty. For a sample containing 3.93 wt% total water, the temperature dependence of the speciation equilibrium can be described by two equations with temperature in K: $\ln k = -36.74/T - 4.02$ for the glass phase (giving enthalpy and entropy of reaction values of $\Delta H = 0.31$ kJ/mol and $\Delta S = -33.45$ J/mol-K), and $\ln k = -3821.83/T + 1.61$ for the melt phase (where $\Delta H = 31.77$ kJ/mol and $\Delta S = 13.41$ J/mol-K) respectively). The glass transition temperature of 670 K is defined by the intersection of these curves. Our values are in good agreement with previously published glass transition temperatures for similar compositions. Similar values for the enthalpy and entropy of reaction were obtained from all the other experiments including those at pressures up to 4.5, 5, and 10 kbars, suggesting that the speciation depends negligibly on pressure for this pressure range.

Introduction

Water is, without a doubt, the most important volatile component in Earth's crust and mantle, and its presence can substantially alter physical and chemical properties of silicate melts including the viscosity, through the depolymerisation of the melt (Burnham 1979). Water is incorporated into silicate melts as both OH groups and molecular H_2O according to the reaction

$$H_2O_{melt} + O_{melt} = 2OH_{melt} \qquad (1)$$

(Stolper 1982a, 1982b; also see review by McMillan 1994). Previous work was performed on silicate glasses quenched from melts, assuming that the speciation in the glass reflected that of the melt at the temperature from which it was quenched (Stolper 1982a). However, Dingwell and Webb (1990) showed that this assumption is incorrect because the relaxation rates in silicate melts above the glass transition temperature (T_g) are so fast that the water speciation cannot be quenched from temperatures above T_g. These authors proposed that the speciation recorded in the glass reflects the equilibrium at the bulk T_g for the system.

Recent advances allow in-situ study of silicate melts and glasses at both temperature and pressure. Specifically, Keppler and Bagdassarov (1993) measured IR spectra of a rhyolite containing 300 ppm water to 1300 °C, and observed changes in the type of OH groups present below the bulk T_g of the system. Nowak (1995), Nowak and Behrens (1995) and Shen and Keppler (1995) reported speciation measurements on silicate glasses at both high temperature and pressure, and found that the speciation did change below T_g. However, Behrens et al. (1998) and Withers and Behrens (in preparation) disagreed with these conclusions, and instead postulated that the changes in band intensities were due to changes in the molar absorption coefficients with temperature. The studies of Shen and Keppler (1995), Nowak (1995), and Nowak and Behrens (1995) have also provided information on the thermodynamics of the reaction obtained from the equilibrium constant for the speciation reaction.

Previous studies concentrated on simple analogue systems such as albite or haplogranite, but few in-situ water speciation studies have been performed on compositions found in nature (Withers et al. 1998; Withers and Behrens, in preparation). Here we present in-situ results from a series of synthetic compositions close to natural rhyolite.

Experimental method

Sample synthesis and preparation

An anhydrous "average" rhyolite glass was prepared from a mixture of SiO_2, Al_2O_3, MgO, $CaCO_3$, Na_2CO_3, K_2CO_3 by heating first to 1200 °C for 24 hours to decarbonate the starting materials then melting at 1600 °C in a Pt crucible for one hour. Microprobe analysis obtained at 15 kV, 10 nA, using a 30 μm spot size gave a total of 98.36 with $SiO_2 = 74.13$, $Al_2O_3 = 13.92$, $K_2O = 5.24$, $Na_2O = 2.90$, CaO = 1.16, MgO = 1.01 wt%. No Fe

*E-mail: John.Sowerby@uni-bayreuth.de

was included in the sample, as this would have produced unwanted crystal field bands in the background of the spectra. The melt was quenched in water and then crushed. Hydrous glasses with between 0 and 5 wt% total water were then prepared by weighing appropriate amounts of anhydrous powder and distilled water into Pt capsules, which were sealed using an electrical arc. These were then placed into an oven at 150 °C overnight, and their weight checked the next day to ensure no water had been lost. The hydrous glasses were synthesised using a rapid quench TZM autoclave at 1100 °C and at pressures of between 1 and 2 kbars for a period of 7 days.

After quenching, the capsules were carefully opened to yield large pieces of hydrous glass. Raman spectroscopy performed on the samples (Zotov and Sowerby, in preparation) did not show any sharp peaks due to the presence of crystalline material in the glass. Part of each sample was then cut and doubly polished to provide 500 μm × 500 μm × 300 μm plates for spectroscopy, with the rest of the sample being used for Karl-Fischer titration, to independently determine the water content (see Behrens et al. 1996 for experimental details). Sample homogeneity was checked by comparing the spectra from several different plates from the same sample. Thicknesses of the polished samples were determined to within ±2 μm. The glass was examined using a Dilor LABRAM micro-Raman spectrometer. We found that small bubbles present in the glass contained CO_2, but that the glass itself lacked CO_2.

Density determination

The density of three water-bearing samples (2.05, 3.08, and 3.93 wt% total water) was obtained by using a Mettler Toledo AG204 balance and their density accessory, using ethanol as the reference fluid, and a density calibration curve obtained from a straight line fitted to these points. Errors in the density are ±5 g/L. To account for the difference in densities between glass and melt, calculations involving data obtained after the glass transition for the sample had their densities reduced by 8% at T_g, as proposed by Nowak and Behrens (1995).

IR spectroscopy

We used a Bruker IFS120HR Fourier transform IR spectrometer, equipped with a microscope. Typically, 100 to 200 scans were collected using a tungsten source, CaF_2 beamsplitter and MCT detector. The resulting spectra were baseline corrected using a flexi-curve style baseline which consists of segments of third-order polynomials fitted through the base line points at 6042, 5413, 4792, 4723, and 4268 cm^{-1} (Fig. 1), and integrated absorbances obtained from the two peaks of interest. To provide an internally consistent data set, the same baseline points were used for all the spectra. We find that this style of baseline is preferable to that employed by Behrens et al. (1996), which in our opinion overestimates the integrated absorbance for the OH peak at 4500 cm^{-1} by a considerable amount, and which also becomes increasingly hard to determine at high temperatures. Comparison of the flexicurve with two straight line baselines, one under each of the peaks, shows a difference of around 1 cm^{-1} in the integrated intensities of both peaks. The flexicurve baseline typically gives relative errors of around ±4–5% in the integrated intensity, increasing to

around ±7% at high temperature. Occasionally for the heating stage and diamond cell experiments, the spectra also displayed a system of large-scale periodic interference fringes. These were removed in one of two ways. For the heating stage experiments, samples which had already been studied at room temperature were used, and these could be subtracted from a room temperature spectrum obtained on the stage, to produce a spectrum containing just the fringes, which could then be removed from the actual spectra. For the diamond cell experiments, fringes were removed by cutting a whole fringe from the spectrum, replicating this at periodic intervals, and then subtracting the resultant spectrum from the sample spectrum.

High-temperature experiments were performed using the heating stage of Zapunnyy et al. (1989), modified by the addition of a Pt plate, in which a hole had been drilled, placed inside the Pt foil heater to support the sample. Temperatures were measured using an Pt/Pt10Rh thermocouple closely attached to the Pt plate. This was calibrated by observing the melting of NaCl, $NaNO_3$, and CsCl. Doubly polished samples could be loaded into the heater, and spectra obtained at high temperature. To verify if water was lost while at high temperature, a spectrum was taken at room temperature after every high-temperature run. If this differed from a previously obtained room temperature spectrum, then the experiment was terminated. The effect of thermal expansion on the glass was assumed to be negligible based on a model calculation using the data from Dingwell et al. (1993) for haplogranite. Over the temperature range studied, the variation in thickness would amount to 0.2%, within the error of the original thickness measurement. The variation in density would be 0.6%. In the evaluation of the spectra, the effects of thermal expansion and thickness partially cancel out. Moreover, density and thickness variations affect the IR bands of OH and H_2O in the same way, i.e., the spectroscopically determined ratio of OH/H_2O is not affected.

Spectra taken simultaneously at high temperature and high pressure were obtained using a hydrothermal diamond anvil cell (Bassett et al. 1993), as modified by Shen and Keppler (1995). Two Mo heaters were employed, produced by winding Mo wire around the tungsten carbide supports for the type I diamonds. Temperatures were measured by chromel-alumel thermocouples attached to the diamonds, and these were calibrated by the same method outlined above. To prevent oxidation of the diamonds and Mo heater, the cell was purged with a gas mixture of 98% Ar and 2% H_2 during high-temperature experiments. The sample chamber in this cell acts as an isochoric system after the initial heating cycle (Bassett et al. 1993). If water is used as the pressure medium, and the homogenization temperature is known, then the bulk density of the water can be obtained. This, along with the equation of state for water, can then be used to obtain the pressure at any temperature.

We placed an irregular chip of hydrous glass into the sample chamber provided by a Re gasket (initial diameter 500 μm, thickness 250 μm), together with water and an air bubble. The cell was then heated, and the fluid phase homogenized. At higher temperatures, typically 600–800 °C, the glass phase melted, and the gasket deformed, a process that was repeated until the melt made contact with both the upper and lower anvils en-

abling FTIR measurements to be taken under hydrostatic conditions but with no interference from the fluid. The diamond cell was cooled, and then transferred to the spectrometer. The cell was then reheated to 900 °C and spectra obtained every 50 °C down to 150 °C. Contact between the upper anvil face and the sample was maintained during cooling, as verified with reflected light. After the experiment, the gasket thickness was obtained by viewing the gasket at 45° in a calibrated binocular microscope. This value provides the sample thickness throughout the experiment.

Reheating the sample until it is in contact with both diamond faces increases its water content. However, during the duration of the spectroscopic measurements, the water content is nearly constant within the experimental error. From the water solubility curve of Holtz et al. (1995) for Ab_{38}-Or_{34}-Qz_{28} we obtained the maximum water content at the highest pressure and temperature reached. This water content provided a density, from the calibration curve obtained earlier. Using this density, an initial estimate of the water content was calculated from the IR data. This water content was then used to correct the density and a final water content for the sample was calculated.

RESULTS

Room temperature

The uncorrected spectra of a series of glasses with different water contents (Fig. 1) have a peak around 5200 cm^{-1} due to the presence of molecular H_2O as a dissolving species in the glass, and a peak at 4500 cm^{-1} assigned to OH groups (see the review by McMillan 1994). Data from all the glasses is shown in Table 1.

Quantitative measurements of the water speciation require the determination of accurate extinction coefficients (Stolper 1982). We used the Beer-Lambert law, rewritten to allow for the two dissolving species as:

$$C_{total} = \frac{1}{\epsilon^*_{OH}} \frac{18.015 A_{OH}}{\rho d} + \frac{1}{\epsilon^*_{H_2O}} \frac{18.015 A_{H_2O}}{\rho d} \quad (2)$$

where C_{total} is the total water concentration, 18.015 the molecular weight of H_2O, A_{OH}, and A_{H_2O} are the integrated absorbances for those two peaks, ϵ^*_{OH} and $\epsilon^*_{H_2O}$ refer to the integrated extinction coefficients in L/mol-cm^2), and ρ and d are the sample density and thickness respectively. Equation 2 can be rewritten as:

$$\frac{C_{total}}{(18.015 A_{OH})/\rho d} = \frac{1}{\epsilon^*_{OH}} + \frac{A_{H_2O}}{A_{OH}} \frac{1}{\epsilon^*_{H_2O}}. \quad (3)$$

By plotting the left hand side of Equation 3 vs. A_{H_2O}/A_{OH} for samples with different water contents (Fig. 2), the two extinction coefficients can be obtained from the y-intercept and the gradient of the line fitted to the data. Values for the extinction coefficients are 263.8 ± 7.4 L/mol-cm^2 for ϵ^*_{OH} and 213.9 ± 4.9 L/mol-cm^2 for $\epsilon^*_{H_2O}$.
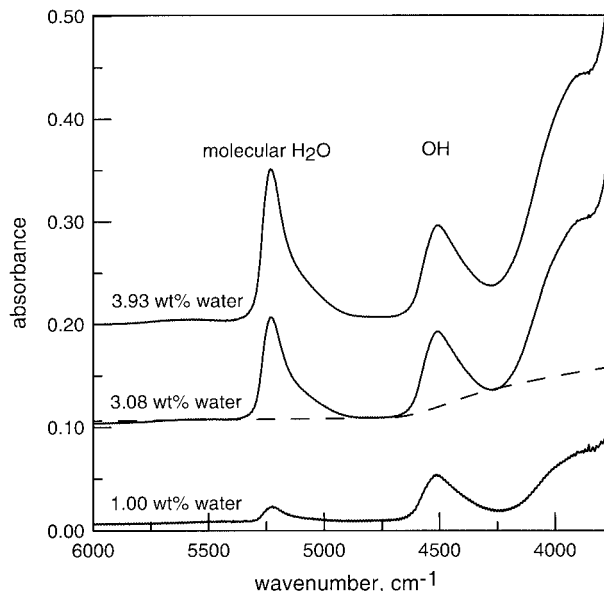

FIGURE 1. Uncorrected near-IR spectra obtained from samples containing different weight percent total water. Sample thickness of each is around 300 µm. Dashed line is an approximate baseline. Spectra are offset sequentially by 0.1 absorbance units for clarity.
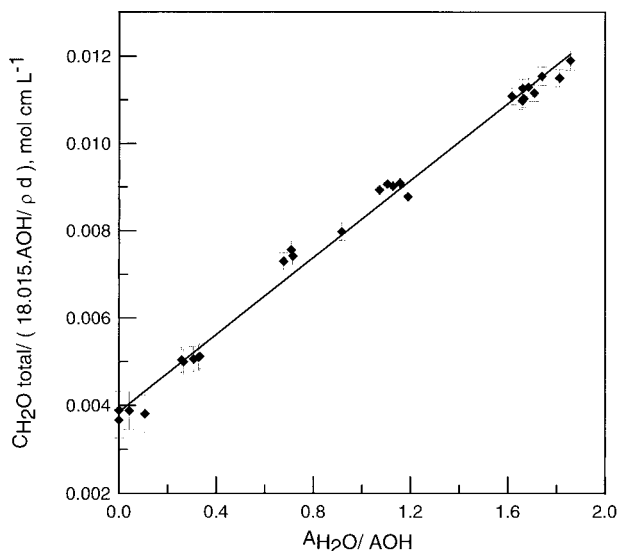

FIGURE 2. Graph used with Equation 3 to determine the integral extinction coefficients for OH and H_2O at room temperature.

TABLE 1. Representative room-temperature spectroscopic data

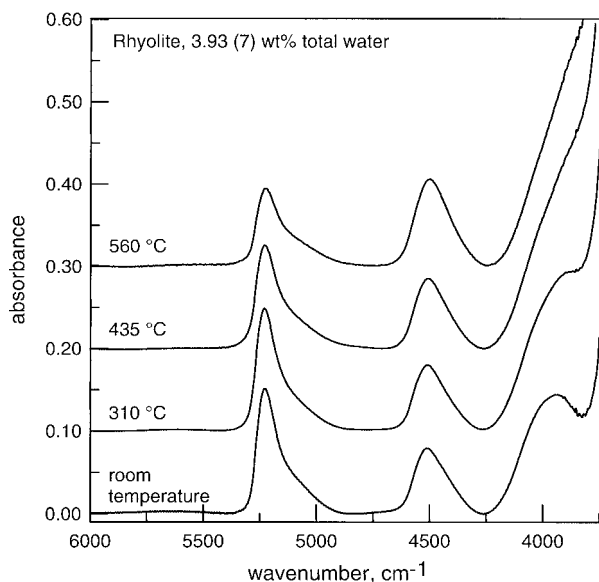| wt% H_2O_{tot}*	Thickness (µm)	OH Absorbance (cm^{-1})	H_2O Absorbance (cm^{-1})	Density (g/L)
4.94 (8)	292	16.3	27.5	2303
3.93 (7)	298	13.7	22.7	2317
3.08 (5)	306	13.9	16.5	2329
2.05 (5)	294	10.6	7.6	2343
1.00 (6)	273	7.0	2.3	2358
0.50 (6)	275	4.6	0	2365
* By Karl Fischer titration.				

FIGURE 3. Baseline corrected NIR spectra obtained from glass containing 3.93 ± 0.07 wt% total water (by Karl-Fischer titration) between room temperature and 560 °C. Changes in the relative intensities of the OH and H$_2$O peaks are evident. Sample thickness was 300 μm. Spectra offset for clarity.

FIGURE 4. A series of spectra obtained from a sample of rhyolite containing 0.5 wt% total water.

High temperature

Figure 3 shows a series of high-temperature spectra. Above 400 °C the intensity of the OH peak at around 4500 cm^{-1} increases with temperature, whereas the intensity of the H$_2$O peak around 5200 cm^{-1} decreases (Table 2). This difference can reflect either an actual change in the speciation with increasing temperature or that the extinction coefficients are changing with temperature. To investigate the cause, a rhyolite containing 0.5 wt% total water, but containing no molecular water, was heated. The variation in integrated intensity for the peak at 4500 cm^{-1} is within the experimental error from room temperature to 865 °C (Fig. 4). We do see the expected shift to lower wavenumbers with increasing temperature. We can conclude that the extinction coefficient for OH does not change. Hence, high-temperature extinction coefficients were obtained from the high-temperature data in Figure 5, using the method outlined earlier. Within the uncertainties of the experiments, we can see no change in the extinction coefficient for H$_2$O with temperature, and in light of the data in Figure 4, we are confident that this holds above 372 °C. Therefore, the variation in the spectra with increasing temperature is the result of a real speciation change, in support of Shen and Keppler (1995), who assumed constant extinction coefficients because a change in temperature of 800 °C should only change the population of the excited vibrational states by 2% or so for such high-energy modes.

Below T_g water speciation is independant of temperature within the uncertainty of the experiment (Fig. 6). However, in support of the previous studies by Nowak and Behrens (1995) and Sh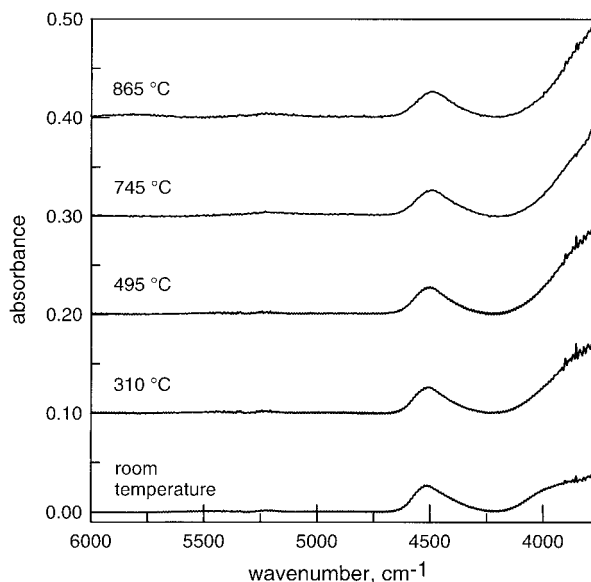en and Keppler (1995), above T_g the concentration of OH rapidly increases and the concentration of molecular H$_2$O concomitantly decreases, such that OH becomes the dominant species around 570 °C. This plot provides additional evidence for the insensitivity of the extinction coefficients to temperature, because the total water content, obtained from the sum of the two species concentrations, stays constant within the experimental error.

High temperature/high pressure

As occurred in the heating stage experiments, the intensity of the OH peak increases with temperature, whereas that of the H$_2$O peak decreases (Fig. 7; Table 3). We propose that this reflects a change in the speciation of water in the sample, with no or very little real change occurring below T_g, and the proportion of OH to H$_2$O increasing rapidly after this point.

DISCUSSION

The speciation data allows the calculation of an equilibrium constant:

$$k = \frac{[OH]^2}{[O] \cdot [H_2O]} \tag{4}$$

assuming ideal mixing, where [OH], [O], and [H$_2$O] are the concentrations of OH, oxygen, and H$_2$O in the melt or glass respectively. Oxygen refers here to all non-protonated oxygen atoms in the sample, whose concentration was obtained by subtracting the concentration of OH and H$_2$O from the total oxygen content derived from the microprobe analysis. The dependence of ln k on reciprocal temperature differs for the
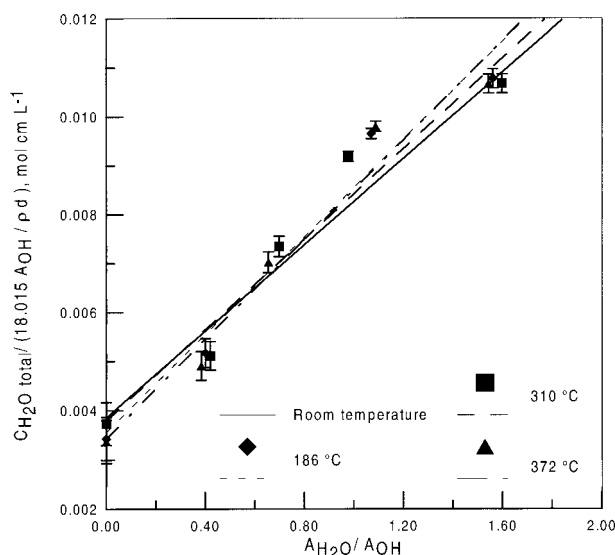
FIGURE 5. Graph showing the negligible effect of temperature on the extinction coefficients. Solid line = results of Figure 2.
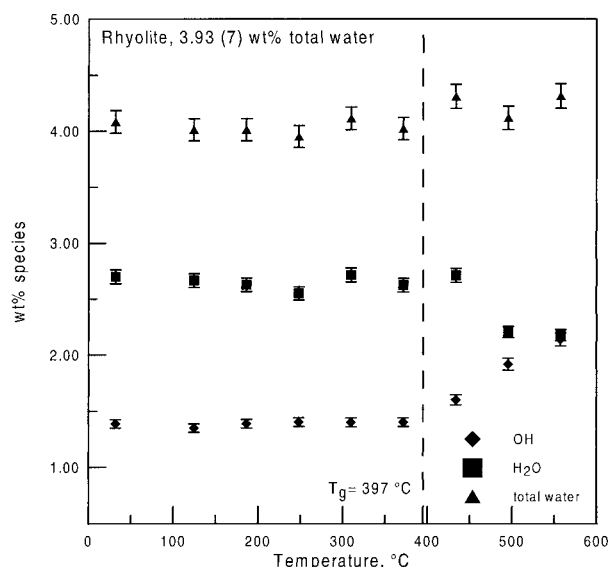

FIGURE 6. Variation of water speciation with temperature for the rhyolite sample in Figure 3. Values were calculated using room temperature extinction coefficients, assuming extinction coefficients do not change. Dashed line is the glass transition for this sample.

TABLE 2. High temperature spectroscopic data, obtained using the heating stage

Temperature (°C)	wt% H_2O*	Thickness (cm)	OH Absorbance (cm^{-1})	H_2O Absorbance (cm^{-1})	Density (g/L)
124	3.93	0.03	13.7	22.2	2317
	3.08	0.0304	12.3	14.5	2329
	2.05	0.0295	10.7	8.1	2343
	1.00	0.0277	7.0	3.0	2358
186	3.93	0.03	14.1	21.9	2317
	3.08	0.0304	12.5	13.4	2329
	2.05	0.0295	10.7	7.5	2343
	1.00	0.0277	7.0	2.8	2358
248	3.93	0.03	14.2	21.3	2317
	3.08	0.0304	12.1	14.4	2329
	2.05	0.0295	10.8	7.6	2343
	1.00	0.0277	7.2	2.6	2358
310	3.93	0.03	14.2	22.7	2317
	3.08	0.0304	13.2	12.9	2329
	2.05	0.0295	10.7	7.5	2343
	1.00	0.0277	7.1	3.0	2358
372	3.93	0.03	14.2	21.9	2317
	3.08	0.0304	12.3	13.4	2329
	2.05	0.0295	11.2	7.3	2343
	1.00	0.0277	7.4	2.8	2358
434	3.93	0.03	14.9	20.8	2132†
	3.08	0.0304	12.6	13.9	2143†
	2.05	0.0295	11.3	7.1	2343
	1	0.0277	7.4	2.8	2358

* By Karl Fischer titration. Errors are the same as in Table 2.
† Density reduced by 8% as described in the text.

glass and melt phases (Fig 8), with the intersection of the two equilibrium curves defining the glass transition temperature of 397 °C. Figure 8 suggests a small change in the water speciation in the glassy state, but within the error of the measurements, this can be considered negligible. The enthalpy and entropy of reaction were determined from fitting ln k vs. $1/T$. The values for the sample with 3.93 wt% H_2O (Table 4), are

very similar to those obtained by Shen and Keppler (1995), Nowak (1995), and Nowak and Behrens (1995) for albitic and haplogranitic melts. Apparently, composition has little influence on the temperature dependence of the speciation reaction in felsic melts.

The equilibrium curves for the melt phase for four sample examined at room pressure and for three different high-pressure
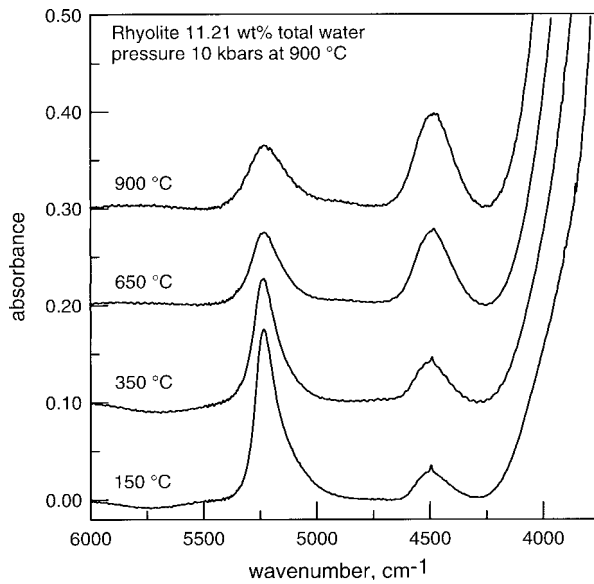
FIGURE 7. Baseline corrected spectra obtained from a rhyolite sample in the diamond anvil cell, at temperature between 150 and 900 °C. The pressure medium had a density of around 0.85 g/cm³ which yields a pressure of around 10 kbars at 900 °C. Sample thickness was 97 μm. Spectra offset for clarity.
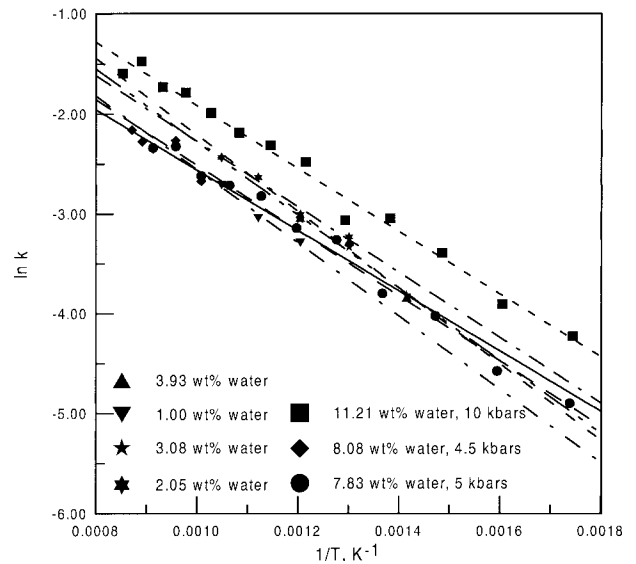

FIGURE 9. Comparison of the temperature dependence of the equilibrium constant for three different melts at high pressure and for four melts at room pressure. (Data given in Tables 2 and 3). Errors in k are around ±8%
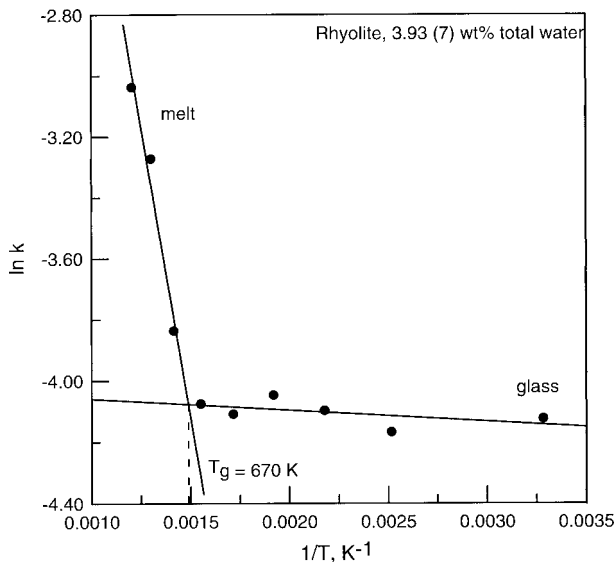

FIGURE 8. Logarithmic dependence of the equilibrium constant k for the reaction $H_2O + O = 2OH$ on inverse temperature. The intersection of the two regression curves gives the glass transition temperature for the sample. For the melt phase, $\ln k = -3821.83/T + 1.61$. For the glass phase, $\ln k = -36.74/T - 4.02$. The relative error in the value of k is ±8%.

FIGURE 10. Dependence of the glass transition temperature on total H_2O content. Dashed curve is haplogranitic and albitic systems (Dingwell 1998).

experiments are nearly parallel (Fig. 9). All yield similar values for the reaction enthalpies and entropies (Table 4). For the pressure range studied, pressure seems to have a negligible affect on the water speciation, in agreement with previous studies (Zhang
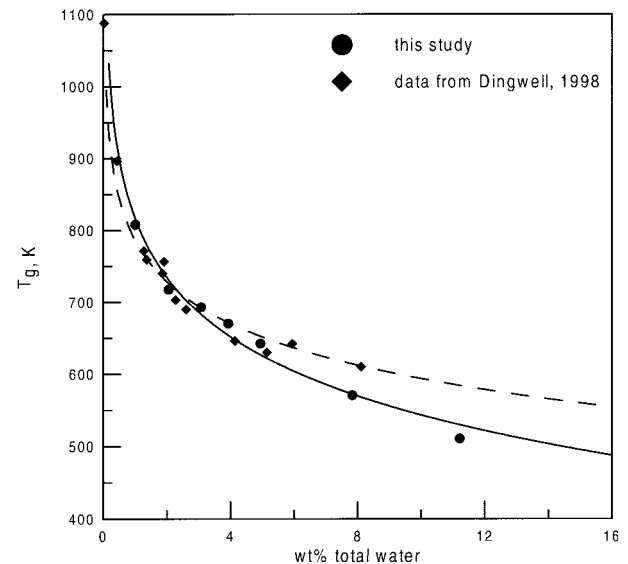
1993; Shen and Keppler 1995; Richet and Polian 1998).

The glass transition temperatures obtained from the speciation data follow a similar trend with total water content as the glasses reported in Dingwell (1998) from both spectroscopic

TABLE 3. Data from the three high-pressure/high-temperature experiments

Expt	Temperature (°C)	OH Absorbance (cm⁻¹)	H₂O Absorbance (cm⁻¹)	Density (g/L)
98001†	150	5.0	26.4	2201
	200	5.5	24.2	2210
	250	4.8	24.7	2211
	300	6.4	21.2	2034*
	350	7.2	19.1	2042*
	400	8.9	17.1	2045*
	450	10.4	16.7	2041*
	500	10.1	15.9	2046*
	550	12.6	13.7	2048*
	600	13.5	13.4	2046*
	650	14.5	14.1	2037*
	700	15.7	13.4	2035*
	750	17.3	13.6	2027*
	800	18.0	14.2	2020*
	850	18.9	11.9	2029*
	900	19.3	14.7	2011*
98003‡	719	14.4	13.9	2087*
	771	17.3	13.5	2080*
	823	17.6	15.5	2072*
	849	17.1	13.3	2081*
	875	18.8	14.7	2071*
98004§	146	5.2	28.4	2249
	198	5.5	26.6	2272
	250	6.1	25.6	2257
	302	6.1	23.8	2074*
	354	7.0	22.4	2077*
	406	8.6	19.4	2083*
	458	9.4	18.1	2086*
	510	11.4	15.4	2089*
	562	12.4	16.6	2082*
	615	13.8	14.9	2084*
	667	14.9	15.7	2078*
	719	14.9	14.2	2083*
	771	17.0	13.9	2078*
	823	17.1	14.4	2076*

* Density reduced by 8% as discussed in text.
† Pressure medium had a density of 0.85 g/cm³, giving a pressure of around 10 kbars at 900 °C. Sample thickness, 0.01 cm.
‡ Pressure medium had a density of 0.67 g/cm³, giving a pressure of around 4.5 kbars at 800 °C. Sample thickness, 0.014 cm.
§ Pressure medium had a density of 0.72 g/cm³, giving a pressure of around 5 kbars at 800 °C. Sample thickness, 0.014 cm.

TABLE 4. Values for ΔH and ΔS obtained for melts from three high pressure and four room pressure experiments

wt% total water	ΔH (kJ/mol)	ΔS, J/(mol-K)
11.21 *	26.15	10.35
8.08 †	25.20	3.94
7.83 ‡	27.17	6.34
3.93 §	31.77	13.41
3.08 §	30.30	11.35
2.05 §	27.21	8.32
1.00 §	30.49	9.25

* Pressure = 10 kbars.
† Pressure = 4.5 kbars.
‡ Pressure = 5 kbars.
§ Room pressure experiment.

and viscosimetric experiments (Fig. 10). Although the T_g values from this study have not been corrected to the 12.38 isokom, (a line of equal viscosity corresponding to a cooling rate of 5K/min) as used by Dingwell (1998), any differences are likely to be negligible, as the cooling rates are similar to those used in previous studies. Note that Dingwell (1998) used a correction of 2 K for the T_g obtained from the diamond cell study of Shen and Keppler (1995), which cooled at 0.28 K/s. The remarkable agreement between the two data sets shows that differences in composition of felsic melts do not change the dramatic effects of hydration.

ACKNOWLEDGMENTS

REFERENCES CITED

Bassett, W.A., Shen, A.H., and Bucknam, M. (1993) A new diamond cell for hydrothermal studies to 2.5 GPa and from –190 to 1200 °C. Reviews of Scientific Instruments, 64, 2340–2345.
Behrens, H., Romano, C., Nowak, M., Holtz, F., and Dingwell, D.B. (1996) Near infrared spectroscopic determination of water species in glasses of the system MAlSi₃O₈ (M = Li, Na, K): an interlaboratory study. Chemical Geology, 128, 41–63.
Behrens, H., Withers, A., and Zhang Y. (1998) In-situ spectroscopy on hydrous albitic and rhyolitic glasses and its implications for water speciation and water species reactions in silicate glasses and melts (extended abstract). Mineralogical Magazine, 62A, 139–140.
Burnham, C.W. (1979) The importance of volatile constituents. In H.S. Yoder, Ed., The Evolution of the Igneous Rocks. Princeton University Press, Princeton, New Jersey
Dingwell, D.B. (1998) The glass transition in hydrous granitic melts. Physics of the Earth and Planetary Interiors, 107, 1–8.
Dingwell, D.B. and Webb, S.L. (1990) Relaxation in silicate melts. European Journal of Mineralogy, 2, 427–449.
Dingwell, D.B., Knoche, R., and Webb, S.L. (1993) The effect of F on the density of haplogranitic melt. American Mineralogist, 78, 325–330.
Holtz, F., Behrens, H., Dingwell, D.B., and Johannes, W. (1995) H₂O solubility in haplogranitic melts: Compositional, pressure and temperature dependence. American Mineralogist, 80, 94–108.
Keppler, H. and Bagdassarov, N.S. (1993) High temperature FTIR spectra of H₂O in rhyolite melt to 1300 °C. American Mineralogist, 78, 1324–1327.
McMillan, P.F. (1994) Water solubility and speciation models. In Mineralogical Society of America Reviews in Mineralogy, 30, 131–156.
Nowak, M. (1995) Der Einbau von Wasser in haplogranitischen Gläsern und Schmelzen, 103 p. PhD dissertation, Universität Hannover.
Nowak, M. and Behrens, H. (1995) An in situ near infrared spectroscopic study of water speciation in haplogranitic glasses and melts. Fifth Silicate Melt Workshop Program and Abstracts, La Petite Pierre, France.
Richet, P. and Polian, A. (1998) Water as a dense icelike component in silicate glasses. Science, 281, 396–398.
Shen, A. and Keppler, H. (1995) Infrared spectroscopy of hydrous silicate melts to 1000 °C and 10 kbar: Direct observation of H₂O speciation in a diamond anvil cell. American Mineralogist, 80, 1335–1338.
Stolper, E. (1982a) The speciation of water in silicate melts. Geochimica Cosmochimica Acta, 46, 2609–2620.
———(1982b) Water in silicate glasses: an infrared spectroscopic study. Contributions to Mineralogy and Petrology, 81, 1–17.
Withers, A.C., Behrens, H., and Holtz, F. (1998) In-situ determination of OH/H₂O speciation in rhyolitic melts using NIR spectroscopy. Terra Abstracts, Abstract supplement No. 1 to Terra Nova, 10, 68.
Zapunnyy, S.A., Sobolev, A.V., Bogdanov, A.A., Slutsky, A.B., Dmitriev, L.V., and Kunin, L.L. (1989) An apparatus for high-temperature optical research with controlled oxygen fugacity. Geochemistry International, 26, 2, 120–128 (translated from Geokhimiya, 7, 1044–1052, 1988).
Zhang, Y. (1993) Pressure dependence of the speciation of water in rhyolitic glasses. Eos (Fall meeting supplement), 74, 631.